

hepth/9304148  
NSF-ITP-93-36

## NUMERICAL ANALYSIS OF BLACK HOLE EVAPORATION

TSVI PIRAN\*

*Center for Astrophysics, Harvard University  
Cambridge, Ma 02138  
and*

ANDREW STROMINGER

*Institute for Theoretical Physics  
and Department of Physics  
University of California  
Santa Barbara, CA 93106-4030*

**ABSTRACT:** Black hole formation/evaporation in two-dimensional dilaton gravity can be described, in the limit where the number  $N$  of matter fields becomes large, by a set of second-order partial differential equations. In this paper we solve these equations numerically. It is shown that, contrary to some previous suggestions, black holes evaporate completely a finite time after formation. A boundary condition is required to evolve the system beyond the naked singularity at the evaporation endpoint. It is argued that this may be naturally chosen so as to restore the system to the vacuum. The analysis also applies to the low-energy scattering of  $S$ -wave fermions by four-dimensional extremal, magnetic, dilatonic black holes.

---

\* On leave from Racah Institute of Physics,  
The Hebrew University, Jerusalem, Israel

In recent work [CGHS], referred to as CGHS, a set of second-order partial differential equations were found to describe both  $1+1$  dimensional black hole formation/evaporation (including backreaction) and scattering of  $S$ -wave matter by  $3+1$  dimensional extremal black holes. The CGHS equations apply to theories of gravity augmented by a scalar dilaton and  $N$  matter fields, and are the first term in a  $1/N$  expansion of the full quantum theory. They provide a concrete arena in which to address the puzzles of quantum mechanical black holes. The CGHS equations apparently are not analytically soluble. Attempts have been made to remedy this problem by modifying the gravity-dilaton couplings. In [ABC] modifications were found which led to exactly soluble (even for finite  $N$ ) quantum theories. Unfortunately these theories are unphysical because the Hamiltonian is unbounded from below [gs]. This difficulty was circumvented in [RST], henceforth referred to as RST, by imposing boundary conditions at the core of the black hole. These boundary conditions ruin the exact solubility of the full quantum theory, but *not* of the large- $N$  semiclassical equations.

A fairly complete picture of black hole evaporation has emerged in the RST model. Black holes evaporate a finite time after formation, and the system can then be restored to the vacuum via an endpoint boundary condition [RST,AS]. Information is destroyed at the spacelike black hole singularity.

While the results of RST are very enlightening, it is still important to try to understand the original CGHS equations. Large  $N$  solubility was obtained in RST at the price of imposing an unnatural global symmetry. One may therefore wonder if the RST results are generic. (Indeed, previous analyses have suggested that solutions of the CGHS equations behave quite differently from those of the RST equations.) In fact we shall see in this paper that most, although not all, of the features of the RST model appear in a more generic setting.

A number of previous attempts have been made to analyse the CGHS equations, but a

definitive conclusion has been surprisingly elusive. It was originally conjectured in CGHS that gravitational collapse did not lead to singularities. This was subsequently shown to be false [BDDO,ORST] in that black hole-like singularities do arise, and static solutions corresponding to a blackhole in equilibrium with a heat bath were found in [husk,nmr]. It was also shown [ORST] that if a large (apparent) black hole is formed, its apparent horizon shrinks due to Hawking evaporation. In [husk] it was suggested that the apparent horizon and singularity approach one another, meeting at future timelike infinity. In [thb] numerical evidence was given that they meet at a finite value of retarded time at future null infinity. This cataclysmic phenomena was referred to as a “thunderbolt”.

In this paper we shall demonstrate numerically that in fact none of these final outcomes are realized. Instead, we find that the apparent horizon and singularity meet in a finite time, in agreement with results of Lowe [LOWE]. A boundary condition is needed at the junction point to continue the evolution of the system. We argue that this boundary condition can be chosen so that the system eventually settles back to the vacuum. However, because a spacelike singularity is present at intermediate stages, information is lost in the process of large  $N$  black hole formation/evaporation.

Two-dimensional dilaton gravity coupled to  $N$  matter fields  $f_i$  is described by the action

$$S = \frac{1}{2\pi} \int d^2\sigma \sqrt{-g} \left[ e^{-2\phi} (R + 4(\nabla\phi)^2 + 4\lambda^2) - \frac{1}{2} \sum_{i=1}^N (\nabla f_i)^2 \right]. \quad (actn)$$

We shall employ conformal gauge in which

$$\begin{aligned} g_{++} &= g_{--} = 0, \\ g_{+-} &= -\frac{1}{2} e^{2\rho}, \end{aligned}$$

where  $\tau^\pm = \tau \pm \sigma$ . In this gauge the “linear dilaton” vacuum solution may be written

$$\begin{aligned} \phi &= \frac{1}{2}(\tau^- - \tau^+), \\ \rho &= 0, \end{aligned} \quad (ldv)$$

where here and henceforth we choose units so that  $\lambda = 1$ . Classical black holes are formed by arbitrary infalling (*i.e.*,  $\partial_- f = 0$ ) matter from  $\mathcal{I}^-$  ( $\tau^- = -\infty$ ). The most general such classical solution is given by

$$\begin{aligned} f &= f(\tau^+), \\ \phi &= -\frac{1}{2} \ln \left[ e^{\tau^+ - \tau^-} - \frac{1}{2} \int e^{\tau^+} \int e^{-\tau^+} \partial_+ f \partial_+ f \right], \\ \rho &= \phi + \frac{1}{2}(\tau^+ - \tau^-), \end{aligned} \quad (csln)$$

or a coordinate transformation thereof. The Penrose diagram for this process is illustrated in Figure 1.

At the quantum level black holes evaporate. In the large  $N$  limit, with  $N e^{2\phi}$  held fixed, the quantum theory is described by the semiclassical CGHS equations. A convenient form of the  $\rho - \phi$  equations is

$$\begin{aligned} 8P\partial_+\partial_-\phi &= -P'(4\partial_+\phi\partial_-\phi + \lambda^2 e^{2\rho}), \\ 2P\partial_+\partial_-\rho &= e^{-4\phi}(4\partial_+\phi\partial_-\phi + \lambda^2 e^{2\rho}), \end{aligned} \quad (rpeq)$$

where

$$\begin{aligned} P &\equiv e^{-4\phi} - \frac{N}{12}e^{-2\phi}, \\ P' &\equiv -4e^{-4\phi} + \frac{N}{6}e^{-2\phi}. \end{aligned} \quad (ppp)$$

These two equations imply the constraint equations, which are given by

$$e^{-2\phi}(4\partial_+\phi\partial_+\rho - 2\partial_+^2\phi) + \frac{1}{2} \sum_{i=1}^N \partial_+ f_i \partial_+ f_i - \frac{N}{12}(\partial_+\rho\partial_+\rho - \partial_+^2\rho) + t_+ = 0, \quad (tpp)$$

together with a similar equation for the  $(--)$  components.  $t_+(t_-)$  is an arbitrary function of  $\tau^+(\tau^-)$  determined by the initial data.

In interpretation of solutions of (rpeq) it is useful to recall [CGHS,BDDO,dxbh] that 1+1 dimensional dilaton gravity may be derived from  $S$ -wave reduction of 3+1 dimensional gravity. In that context  $4\pi e^{-2\phi}$  measures the area of the two spheres of constant radius [dxbh]. Correspondingly a future (past) apparent horizon is a line along which  $\partial_+\phi(\partial_-\phi)$

vanishes[ORST]. (This is distinct from the event horizon, which is a null line from behind which one cannot escape to  $\mathcal{I}^+$ .) This apparent horizon provides a useful two-dimensional definition of the boundary of a black hole.

In the classical theory, the kinetic terms in the action degenerate at  $e^{-2\phi} = 0$ , which may be thought of as the origin since the two spheres have zero area. In the large  $N$  quantum theory this degeneration occurs at the finite value  $\phi_{cr}$  of  $\phi$  such that  $e^{-2\phi_{cr}} = \frac{N}{12}$ , as can be seen from inspection of (rpeq). Thus the quantum mechanical origin is at  $\phi_{cr}$ , and we shall not try to evolve the system beyond this point.

We first compute the effects of sending in a shock wave of infalling matter along  $\tau^+ = 0$  with total energy  $M$ . Initial value data for this problem may consist of the values of  $\rho$  and  $\phi$  along two orthogonal null lines. We specify vacuum data along  $\tau^+ = 0$ :

$$\begin{aligned} \rho(0, \tau^-) &= 0, \\ \phi(0, \tau^-) &= \frac{1}{2}\tau^-. \end{aligned} \tag{vdta}$$

Along  $\mathcal{I}^-$ , the quantum equations exponentially approach the classical equations, and the initial data should agree with the classical solution (csln) with  $\frac{1}{2}\partial_+ f \partial_+ f = M\delta(\tau^+)$ :

$$\begin{aligned} \tau^+ &> 0, \\ \tau^- &\rightarrow -\infty, \\ \phi &\rightarrow -\frac{1}{2}\ln\left[M(1 - e^{\tau^+}) + e^{\tau^+ - \tau^-}\right], \\ \rho &\rightarrow \phi + \frac{1}{2}(\tau^+ - \tau^-). \end{aligned} \tag{asdt}$$

Of course it is not possible numerically to set initial data at  $\tau^- = -\infty$ . Instead we specify the data at a large negative value  $\tau_0^-$  of  $\tau^-$ ;

$$\begin{aligned} \tau^+ &> 0, \\ \phi_0 &= -\frac{1}{2}\ln\left[M(1 - e^{\tau^+}) + e^{\tau^+ - \tau_0^-}\right], \\ \rho_0 &= \phi + \frac{1}{2}(\tau^+ - \tau_0^-), \end{aligned} \tag{appr}$$

which induces an error of order  $e^{\tau_0^-}$ . We then check numerically for convergence at large negative  $\tau_0^-$ .<sup>†</sup>

Our code approximates the spacetime using a null grid in  $\tau^\pm$ . It computes the variables in some preset range  $0 < \tau^+ < \tau_{MAX}^+$  and then steps up in  $\tau^-$ . The numerical computation cannot continue past a point where  $\phi = \phi_{cr}$ , so it is instructed to revert to  $\tau^+ = 0$  and integrate along the next  $\tau^-$  step until the singularity is again encountered. In this way it fills in the region under (but not in the causal shadow of) the singularity.

The results are plotted for  $M = .5$  and  $N = 12$  in figures 2a, 2b and 2c. Since  $N$  may be scaled out of the equations by shifting  $\phi$  the results are qualitatively independent of  $N$ . A black hole (*i.e.*, a region where  $\partial_+\phi > 0$ ) forms a finite distance along the infall line. A spacelike singularity is produced when the shockwave reaches the origin where  $\phi = \phi_{cr}$  ( $\phi_{cr} = 0$  for  $N = 12$ ). All future-directed ingoing null geodesics inside the black hole terminate at the singularity. The apparent horizon becomes timelike due to Hawking radiation. Our computation clearly indicates that (contrary to previous claims) the apparent horizon meets the singularity in a finite proper time. At this “endpoint” denoted  $(\tau_E^+, \tau_E^-)$ , the black hole has shrunk to zero size (as measured by  $e^{-2\phi} - \frac{N}{12}$ ).

The endpoint singularity is visible to observers outside the black hole with coordinates  $\tau^\pm \geq \tau_E^\pm$ , so this constitutes a violation of cosmic censorship. Boundary conditions are required to evolve the system beyond the endpoint. Physically one expects that it should be possible to impose boundary conditions which restore the system to near-vacuum just after the endpoint. Indeed, inspection of Figure 3 shows that along the edge of the causal shadow of the singularity ( $\tau^+ > \tau_E^+, \tau_E^-$ ), the fields are very near their vacuum values. However, they are not *exactly* equal to their vacuum values. This is also expected: the outgoing Hawking radiation itself induces particle production. This leads to some flux crossing the line ( $\tau^+ > \tau_E^+, \tau_E^-$ ) along which the black hole is seen to disappear.

---

<sup>†</sup> Erroneous conclusions were reached in [thb] as a result of choosing a small value of  $\tau_0^-$ .

Potentially this infalling energy flux could recollapse to form a new black hole. However, we do not think that this is the case, because dilaton black holes (of all sizes) radiate energy at a rate of order  $N/48$ <sup>†</sup>. Therefore there is a threshold for black hole production: energy must be thrown in faster than it is radiated away. Such a threshold was found analytically in the RST model, and numerical evidence for the existence of a similar threshold in the CGHS model is illustrated in figures 4 and 5.

Although presumably no black hole is formed below the threshold, (*i.e.*,  $\partial_+\phi < 0$  everywhere), the CGHS equations are still ill-defined at  $\phi = \phi_{cr}$ . However since this is a timelike line, it is presumably possible to choose reflecting boundary conditions so that the below-threshold radiation passes through the origin without collapsing.

A plausible picture of black hole formation in the CGHS model is thus the following. The black hole evaporates completely in a finite time and, with the help of an endpoint boundary condition, disappears completely. Weak, backscattered, infalling radiation remains, but this can be reflected through the origin. The excitations eventually dissipate and the system settles back down to the linear dilation vacuum. The Penrose diagram is illustrated in Figure 6.

The CGHS model differs from the RST model in this last respect: In the case of RST, there is no backscattered radiation, and the system is identically vacuum in the causal future of the black hole endpoint. This appears to be a non-generic feature of the RST model, perhaps associated with the unnatural symmetries.

We have also considered the semiclassical one-loop ghost-corrected equations derived in [fpbh], and given by (rpeq) with the first equation in (ppp) replaced by

$$P = e^{-4\phi} - \frac{N}{12}e^{-2\phi} + \frac{N}{24}. \quad (pfb)$$

---

<sup>†</sup> The black hole mass  $M$  is also of order  $N$  with our conventions.

The extra term in (pb) moves the critical values of  $\phi$  into the complex plane and eliminates the singularity. The behavior of the system was analyzed in [fpbh]. In particular it was shown that the static solutions describe black holes with non-singular, asymptotically deSitter interiors in thermal equilibrium with a bath of Hawking radiation. A numerical simulation of shock wave collapse described by these equations is illustrated in Figure 7. A more detailed analysis is required to fully understand this system, but it appears that the shock wave creates a black hole which subsequently evaporates down to a stable remnant with a deSitter-like interior. It is apparently possible to create a remnant with an arbitrarily weak shock wave, which indicates that the remnant mass may be less than the linear dilaton vacuum.

#### Acknowledgements

This work was supported in part by DOE grant DEAC-03-8ER4050, NSF grant PHY89-04035 and the US-Israel BSF foundation. We are grateful to B. Birnir and D. Goldwirth for useful conversations. We also acknowledge the Aspen Center for Physics, where this work was initiated.

#### REFERENCES

LOWE. D.A. Lowe, “Semiclassical Approach to Black Hole Evaporation” *Phys. Rev.* **D47**,(1993) 2446.

CGHS. C.G. Callan, S.B. Giddings, J.A. Harvey and A. Strominger, “Evanescent Black Holes”, *Phys. Rev.* **D45**, R1005, (1992); For recent reviews see J.A. Harvey and A. Strominger, “Quantum Aspects of Black Holes” preprint EFI-92-41, hep-th@xxx/9209055, to appear in the proceedings of the 1992 TASI Summer School in Boulder, Colorado, and S.B. Giddings, “Toy Models for Black Holes Evaporation” preprint UCSBTH-92-

36, hep-th@xxx/9209113, to appear in the proceedings of the International Workshop of Theoretical Physics, 6th Session, June 1992, Erice, Italy.

BDDO. T. Banks, A. Dabholkar, M.R. Douglas, and M. O'Loughlin, “Are horned particles the climax of Hawking evaporation?” *Phys. Rev.* **D45**, (1992) 3607.

dxbh. S.B. Giddings and A. Strominger, “Dynamics of Extremal Black Holes”, *Phys. Rev.* **D46**, (1992) 627.

fpbh. A. Strominger, “Fadeev-Popov ghosts and  $1+1$  dimensional black hole evaporation”, *Phys. Rev.* **D46**, (1992) 4396.

gs. S. Giddings and A. Strominger, “Quantum theories of dilaton gravity”, *Phys. Rev.* **D46** (1993) 2454.

ORST. J.G. Russo, L. Susskind and L. Thorlacius, “Black Hole Evaporation in  $1+1$  Dimensions”, *Phys. Lett.* **B292**, 13 (1992).

thb. S.W. Hawking and J.M. Stewart, “Naked and thunderbolt singularities in black hole evaporation”, hep-th/9207105.

AS. A. Strominger, unpublished.

RST. J.G. Russo, L. Susskind, and L. Thorlacius, *Phys. Rev.* **D46** (1992) 3444.

husk. L. Susskind, and L. Thorlacius, “Hawking radiation and backreaction”, *Nucl. Phys.* **B382** (1992) 123.

nmr. S.W. Hawking, “Evaporation of two dimensional black holes”, *Phys. Rev. Lett.* **69**, (1992) 406; B. Birnir, S. Giddings, J. Harvey and A. Strominger, “Quantum Black Holes”, *Phys. Rev.* **D46**, (1992) 638.

ABC. A. Bilal and C. Callan, “Liouville models of black hole evaporation”, Princeton preprint PUPT-1320, hep-th/9205089; S.P. deAlwis, “Quantization of a theory of

2d dilaton gravity”, Boulder preprint COLO-HEP-280, hep-th/9205069, “Black hole physics from Liouville theory”, Boulder preprint COLO-HEP-284, hep-th/9206020, “Quantum Black Holes in Two Dimensions”, Boulder preprint COLO-HEP-288, hep-th/9207095.

## FIGURE CAPTIONS

**Figure 1.** Penrose diagram for classical black hole formation by an  $f$  shock wave with stress tensor  $\frac{1}{2}\partial_+f\partial_+f = M\delta(\tau^+ - \tau_0^+)$ .

**Figures 2a, 2b, 2c.** Numerical simulation of black hole formation and evaporation. Initial conditions are specified along the left and lower boundaries of the plot corresponding to a null  $M = .5$  shock wave along the left boundary. The contours in Figure 2a depict lines of constant  $\phi$  (the rippled dashes are an artifact of the plotting routine). The interior of the black hole is the region where these lines slope downward to the right, and the apparent horizon is the boundary of this region. The results depicted here depend on two numerical parameters:  $\tau_0^-$ , the initial  $\tau^-$  value, and  $d\tau$ , the numerical time step. In order to ensure that the results are not due to numerical errors we checked the convergence of our results as  $\tau_0^- \rightarrow -\infty$  and  $d\tau \rightarrow 0$ . In Figure 2b we depict the singularity line  $\phi = \phi_{cr}$  and the apparent horizon line  $\partial_+\phi = 0$  for  $d\tau$  values ranging between  $4 \cdot 10^{-3}$  and  $6.25 \cdot 10^{-5}$ . It is evident that the curves converge. More quantitative tests show that the errors decrease like  $d\tau^2$  and  $e^{\tau_0^-}$ , as expected.

Figure 2b suggests that singularity and the horizon intersect. However, technically, our scheme cannot reach the intersection point  $(\tau_E^+, \tau_E^-)$  itself. The numerical scheme breaks down and it is impossible to continue the computation in the  $\tau^+$  direction when  $\phi = \phi_{cr}$ . Regardless of how fine our resolution is we can never reach the endpoint  $(\tau_E^+, \tau_E^-)$ . There will always be a gap of one computation step  $d\tau$  between the last  $\tau^-$  value for which we calculated the horizon's position and the first  $\tau^-$  that is singular. However, Figure 2c shows an enlargement of the region near  $(\tau_E^+, \tau_E^-)$ . The different points correspond to the two finest (smallest  $d\tau$ ) computations and the curves describe a Pade extrapolation through these points. The agreement between the computed points demonstrates the numerical convergence of our computation. The fact that the extrapolated curves intersect, at a

point just beyond the end of the computation, is clear evidence that  $(\tau_E^+, \tau_E^-)$  exist and are near  $(.3154, -.1093)$ .

**Figure 3.** Numerical simulation of black hole formation and evaporation. Initial conditions are specified along the left and lower boundaries of the plot corresponding to a null  $M = .5$  shock wave along the left boundary. This plot extends to larger values of  $\tau^+$  than those appearing in Figure 2a. It is evident that lines of constant  $\phi$  cross into the causal shadow of the black hole endpoint along  $\tau_E^- \sim -0.1$ . The nearly straight nature of those lines for large  $\tau^+$  also indicates that the system is near its vacuum configuration far from the black hole.

**Figure 4.** Energy is thrown towards the origin at a constant, above-threshold rate for  $\tau^+ > 0$ , corresponding to a matter stress tensor  $\frac{1}{2}\partial_+f\partial_+f = \theta(\tau^+)$ . A black hole forms and grows because matter accretion outpaces Hawking radiation. A spacelike singularity eventually crosses the null line  $\tau^- = 0$  where the numerical simulation ends.

**Figure 5.** Energy is thrown towards the origin at a constant, below-threshold rate for  $\tau^+ > 0$ , corresponding to a matter stress tensor  $\frac{1}{2}\partial_+f\partial_+f = .5\theta(\tau^+)$ . A black hole does not form because Hawking radiation outpaces matter accretion. No singularity crosses the null line  $\tau^- = 0$  where the numerical simulation ends.

**Figure 6.** Conjectured Penrose diagram for large- $N$  black hole formation/evaporation. The black hole disappears in a finite time. Boundary conditions can be chosen along the timelike segment of the line  $\phi = \phi_{cr}$  after the endpoint in such a way that the system eventually settles back down to the vacuum.

**Figure 7.** Numerical simulation of black hole formation and evaporation, as described by the one-loop ghost-corrected semiclassical equations with  $N = 12$ . Initial conditions are specified along the left and lower boundaries of the plot corresponding to a null  $M = .1$  shock wave along the left boundary. The contours depict lines of constant  $\phi$ . The

simulation is terminated when  $e^{2\rho}$  diverges. This is apparently a coordinate divergence at an infinite distance away from finite points in the spacetime, indicating the possible formation of a deSitter-like region inside the horizon. For large  $\tau^+$  the system appears to settle down to a static remnant.

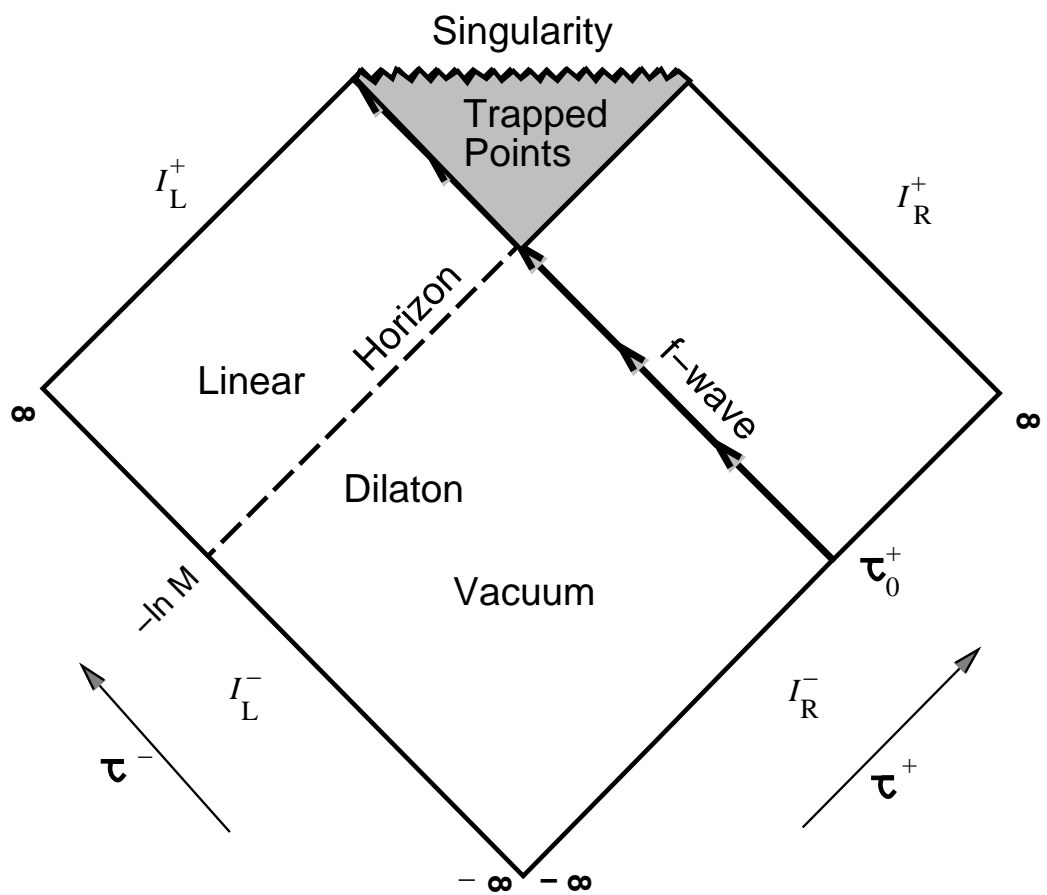


Fig. 1

Fig. 2a

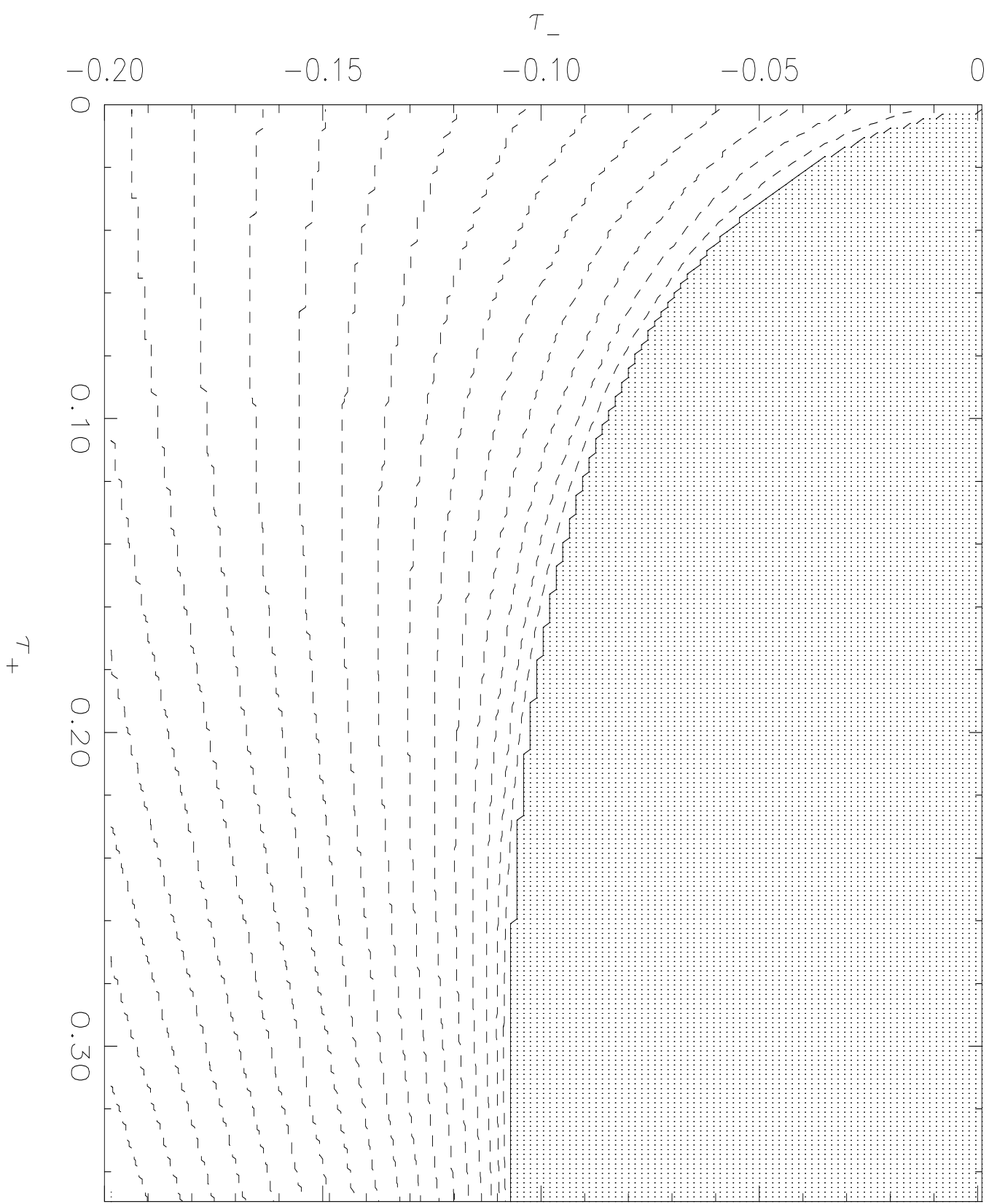


Fig. 2b

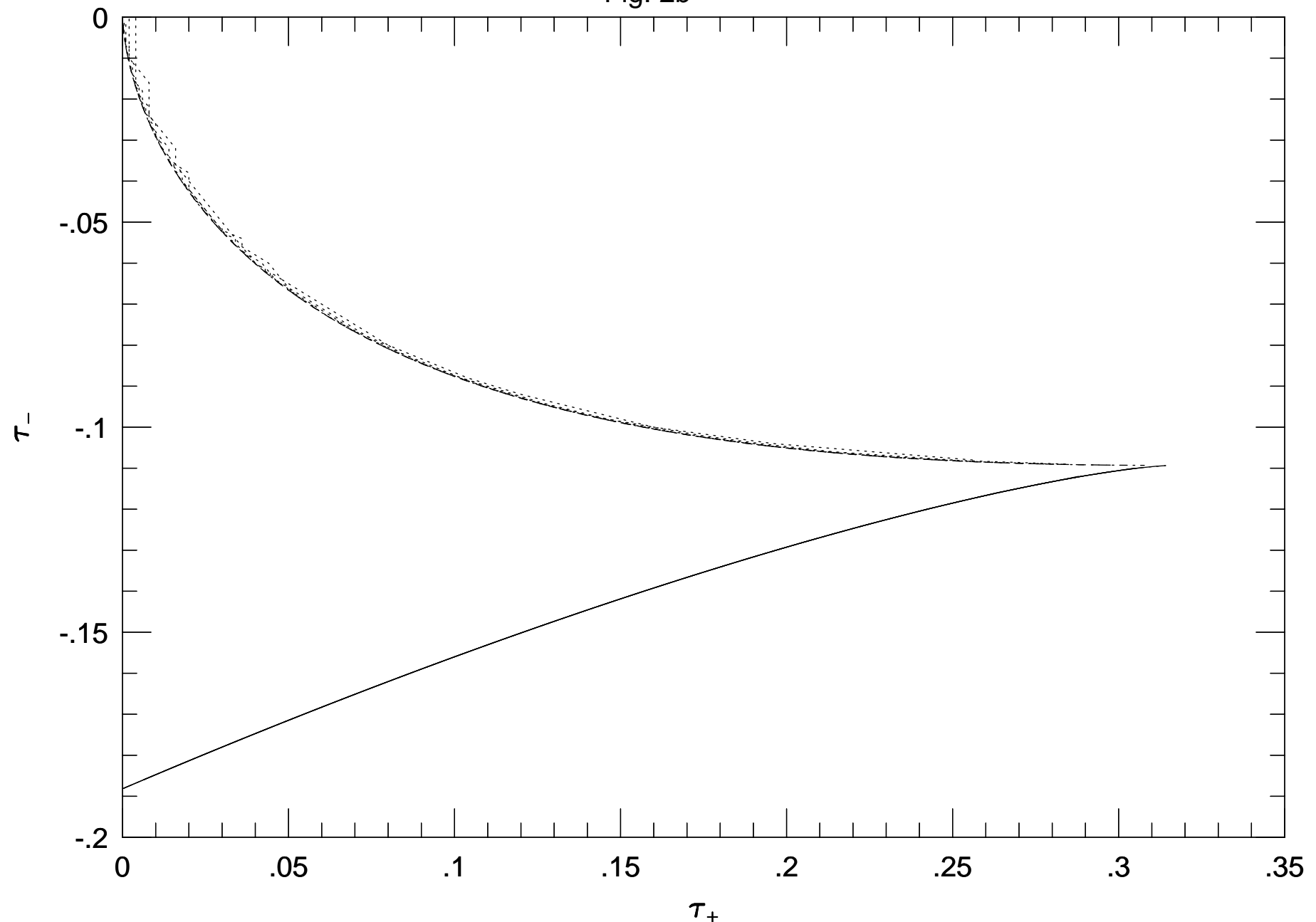


Fig 2c

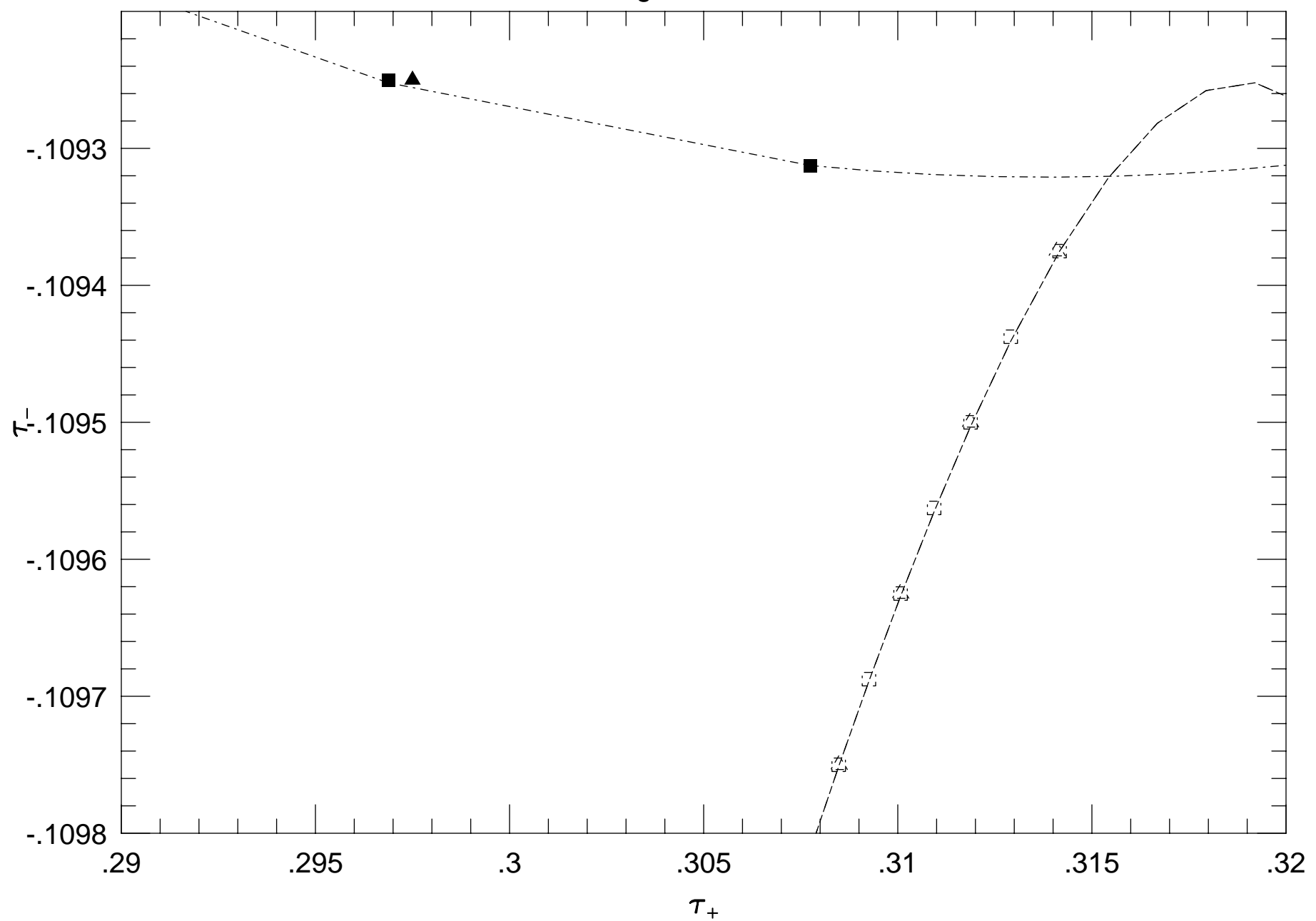


Fig. 3

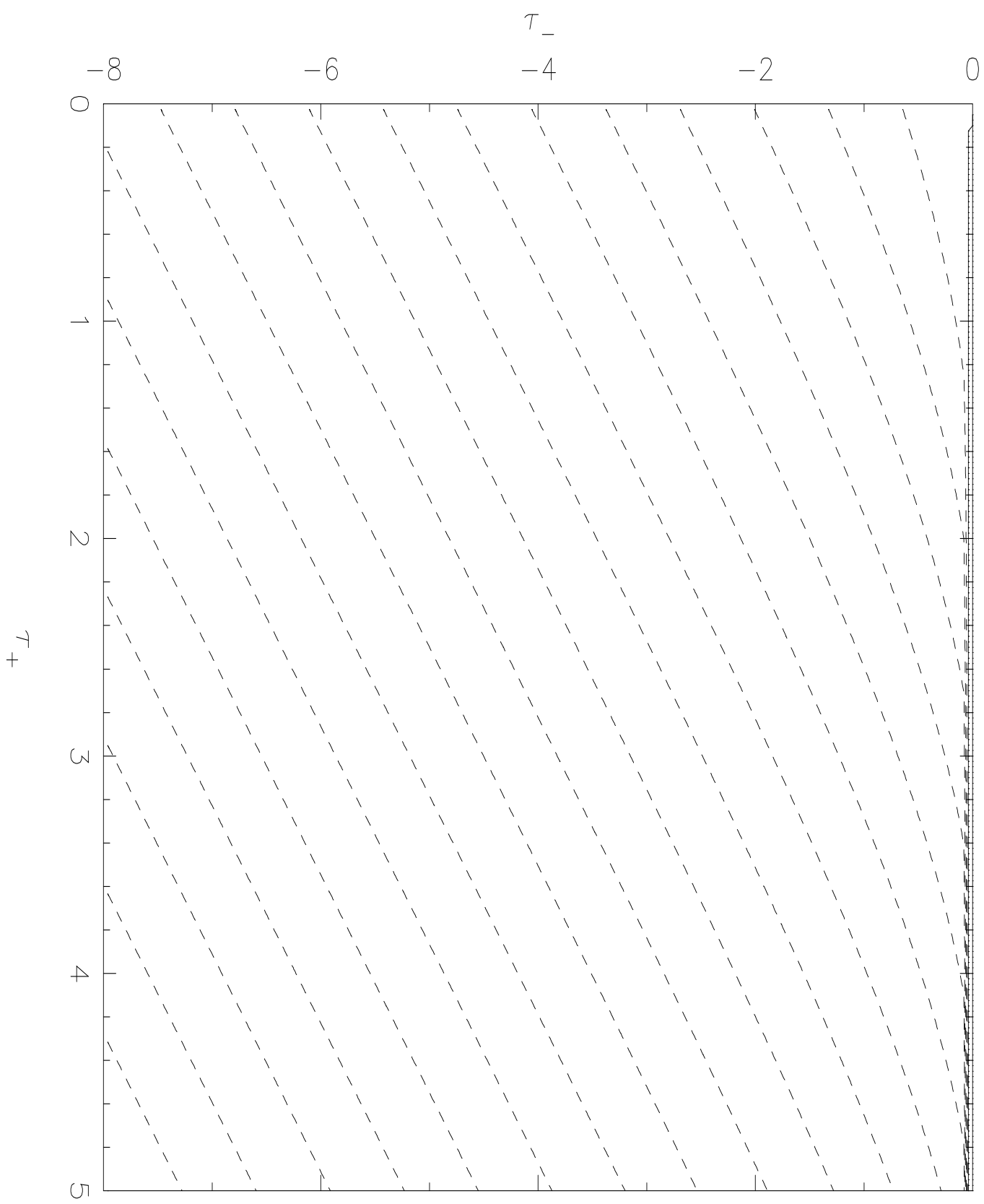


Fig. 4

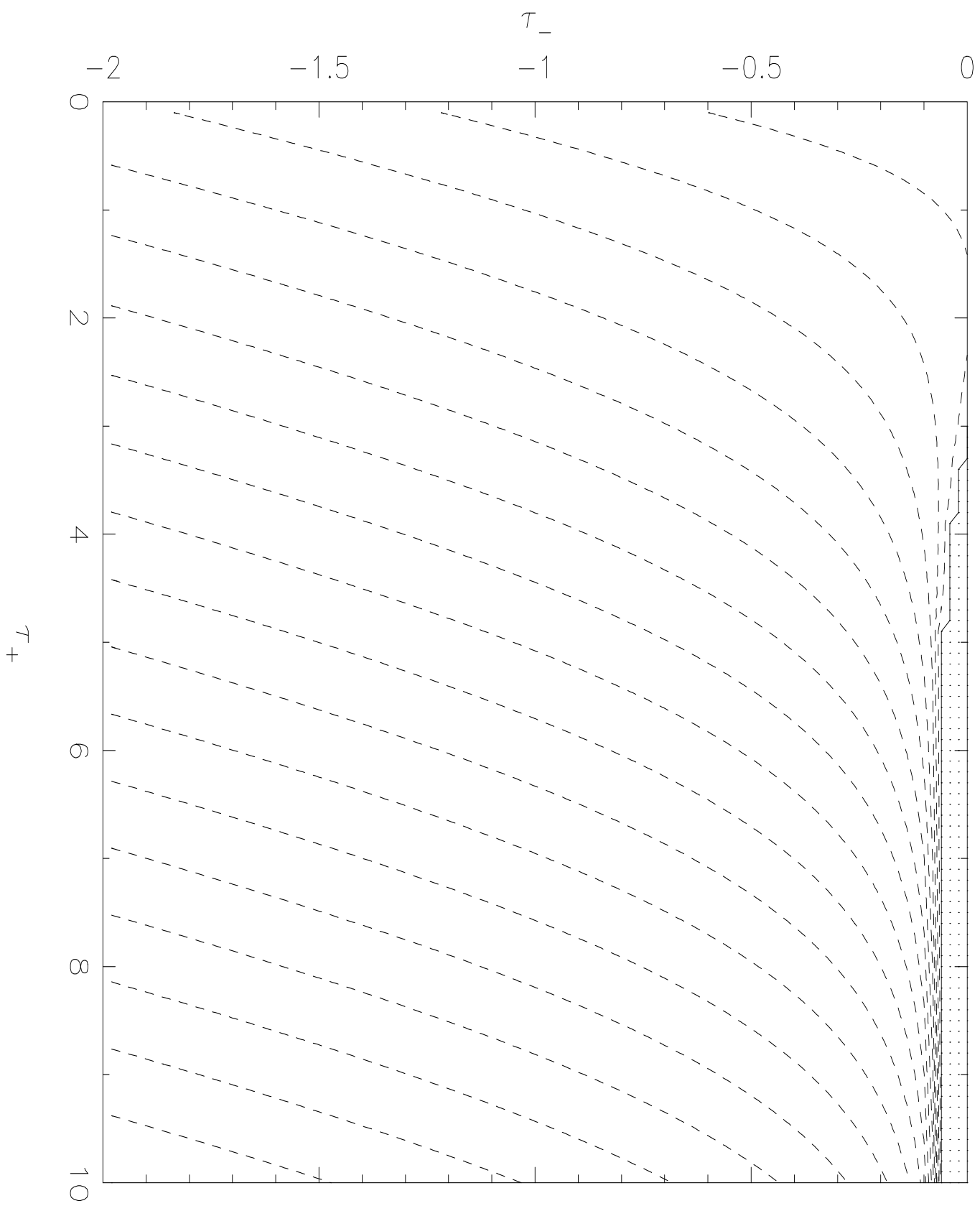
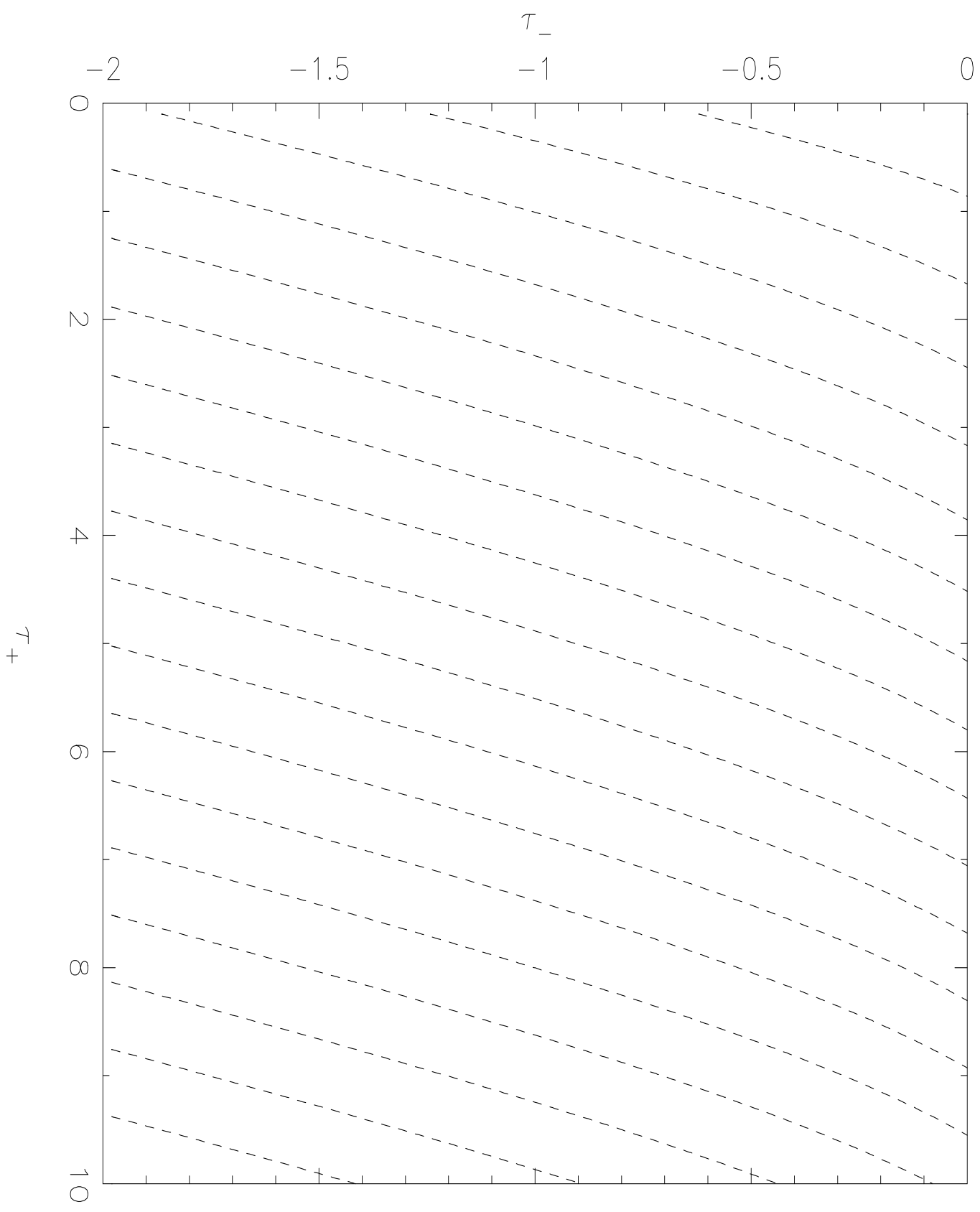
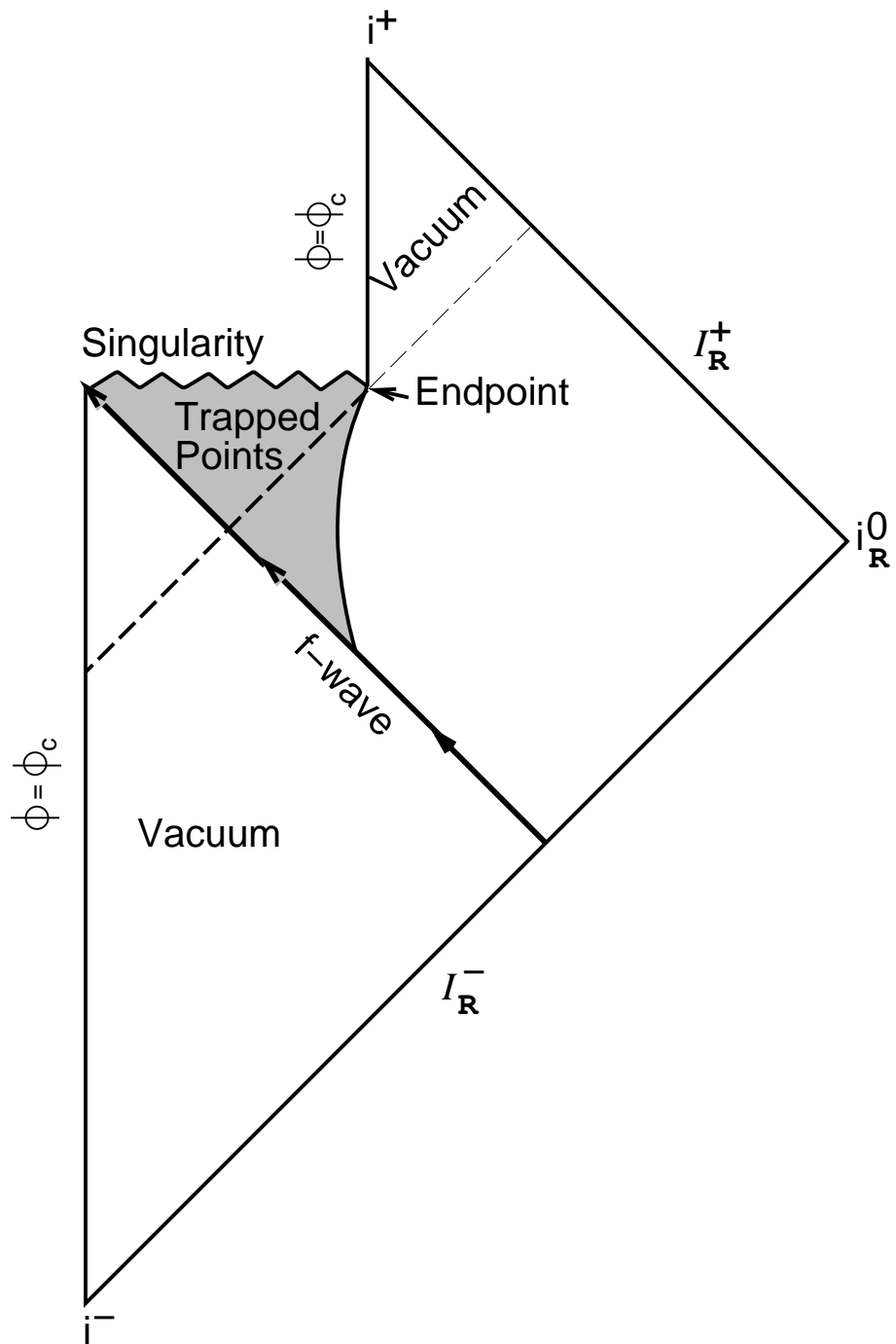


Fig. 5





**Fig. 6**

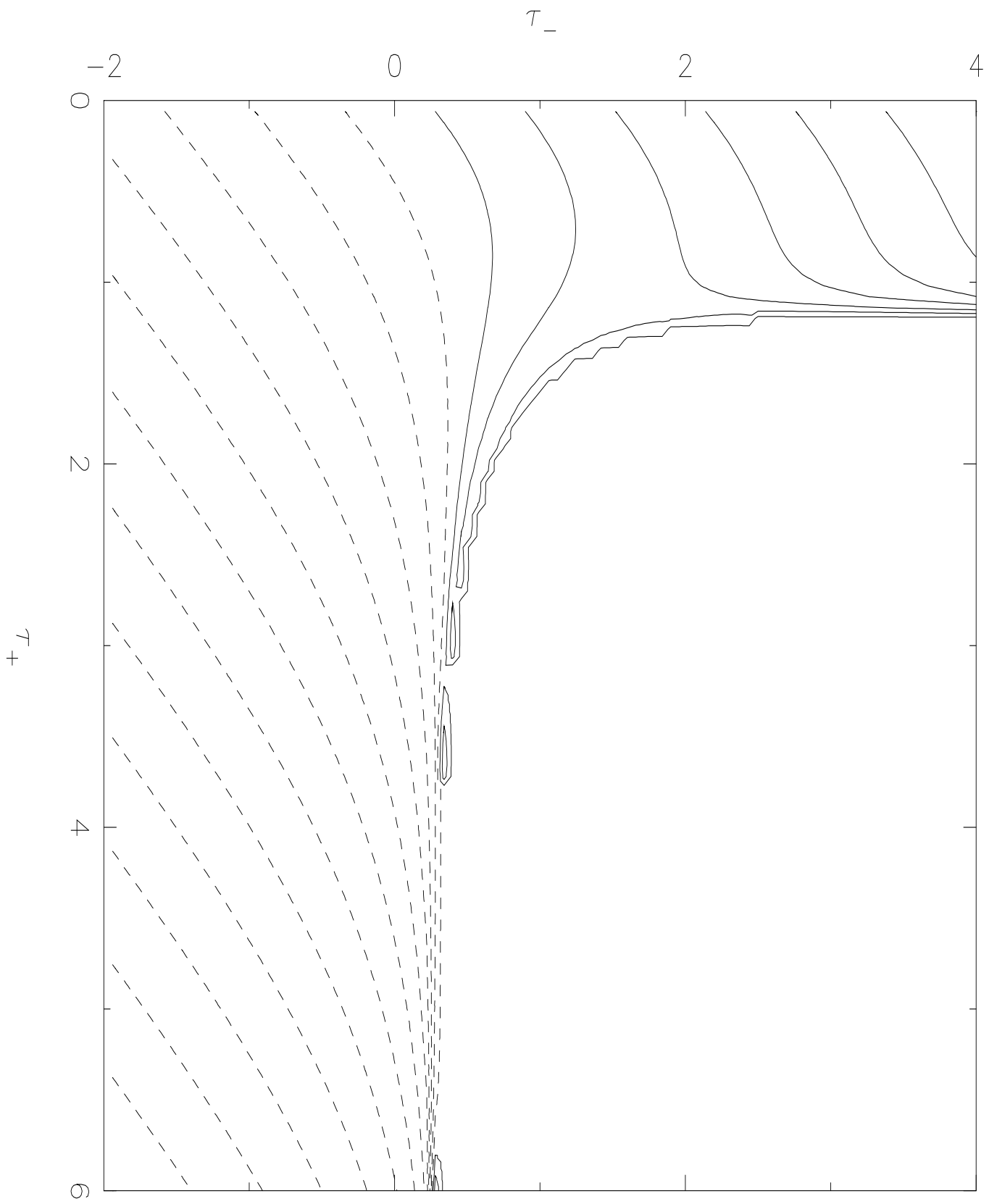


Fig. 7